

Search for Violations of Lorentz Invariance and CPT Symmetry in $B_{(s)}^0$ MixingR. Aaij *et al.**

(LHCb Collaboration)

(Received 16 March 2016; published 15 June 2016)

Violations of CPT symmetry and Lorentz invariance are searched for by studying interference effects in B^0 mixing and in B_s^0 mixing. Samples of $B^0 \rightarrow J/\psi K_S^0$ and $B_s^0 \rightarrow J/\psi K^+ K^-$ decays are recorded by the LHCb detector in proton-proton collisions at center-of-mass energies of 7 and 8 TeV, corresponding to an integrated luminosity of 3 fb^{-1} . No periodic variations of the particle-antiparticle mass differences are found, consistent with Lorentz invariance and CPT symmetry. Results are expressed in terms of the standard model extension parameter Δa_μ with precisions of $\mathcal{O}(10^{-15})$ and $\mathcal{O}(10^{-14})$ GeV for the B^0 and B_s^0 systems, respectively. With no assumption on Lorentz (non)invariance, the CPT -violating parameter z in the B_s^0 system is measured for the first time and found to be $\text{Re}(z) = -0.022 \pm 0.033 \pm 0.005$ and $\text{Im}(z) = 0.004 \pm 0.011 \pm 0.002$, where the first uncertainties are statistical and the second systematic.

DOI: [10.1103/PhysRevLett.116.241601](https://doi.org/10.1103/PhysRevLett.116.241601)

Lorentz invariance and the combination of charge conjugation, spatial inversion, and time reversal (CPT) are exact symmetries in the standard model (SM) of particle physics, and are deeply connected in any quantum field theory [1]. Quantum theories that aim to describe Planck-scale physics, such as string theory, might break these fundamental symmetries [2]. Present-day experiments are many orders of magnitude away from the Planck energy scale of $\sim 10^{19}$ GeV; however, small effects at low energy might still be observable. Interference effects in the mixing of neutral mesons are sensitive to violations of CPT symmetry, and therefore may provide a window to the quantum gravity scale [3]. Such effects can be quantified in a low-energy, effective field theory, as done in the standard model extension (SME) [4,5]. In this framework, terms that explicitly break Lorentz and CPT symmetry are added to the SM Lagrangian to describe the couplings between particles and (hypothetical) uniform tensor fields. These fields would acquire nonzero vacuum expectation values when these symmetries are spontaneously broken in the underlying theory. The SME couplings are expected to be suppressed by powers of the Planck scale [6]. In the SME, the CPT -violating parameters that can be measured in neutral meson systems also break Lorentz symmetry. The amount of CPT violation depends on the direction of motion and on the boost of the particle. The SME parameters for the B^0 and B_s^0 systems can be best measured with a time-dependent analysis of the decay channels $B^0 \rightarrow J/\psi K_S^0$ and $B_s^0 \rightarrow J/\psi K^+ K^-$, using the four-velocity of the

B mesons [7]. The notation B refers to either B^0 or B_s^0 and the inclusion of charge-conjugate processes is implied throughout this Letter. These parameters have been measured previously, albeit with less sensitive decay modes [7], by the BABAR collaboration for the B^0 system [8], and by the D0 collaboration for the B_s^0 system [9].

The LHCb detector is a single-arm forward spectrometer described in detail in Refs. [10,11]. Simulated events are produced using the software described in Refs. [12–16]. The data used in this analysis correspond to an integrated luminosity of 3 fb^{-1} , taken at the LHC at proton-proton center-of-mass energies of 7 and 8 TeV. The selection of both decay channels is the same as used in Refs. [17] and [18]. The J/ψ meson is reconstructed in the dimuon channel and the K_S^0 meson in the $\pi^+ \pi^-$ final state.

Interference effects from CPT violation can be incorporated generically in the time evolution of a neutral B meson system, described by the Schrödinger equation $i\partial_t \Psi = \hat{H} \Psi$. The effective 2×2 Hamiltonian is written as $\hat{H} = \hat{M} - i\hat{\Gamma}/2$ [19]. Diagonalization gives a heavy-mass eigenstate $|B_H\rangle$ and a light-mass eigenstate $|B_L\rangle$ with masses $m_{H,L}$ and decay widths $\Gamma_{H,L}$. The differences between the eigenvalues are defined as $\Delta m \equiv m_H - m_L$ and $\Delta \Gamma \equiv \Gamma_L - \Gamma_H$. The differences between the diagonal matrix elements of the effective Hamiltonian are defined as $\delta m \equiv M_{11} - M_{22}$ and $\delta \Gamma \equiv \Gamma_{11} - \Gamma_{22}$. Any difference between the mass or lifetime of particles and antiparticles (i.e., a nonzero δm or $\delta \Gamma$) is a sign of CPT violation, and is characterized by

$$z = \frac{\delta m - i\delta \Gamma/2}{\Delta m + i\Delta \Gamma/2}, \quad (1)$$

and the mass eigenstates are given by $|B_{H,L}\rangle = p\sqrt{1 \pm z}|B\rangle \mp q\sqrt{1 \mp z}|\bar{B}\rangle$. Owing to the smallness of the B mixing parameters Δm and $\Delta \Gamma$ in the denominator, z is highly sensitive to CPT -violating effects.

*Full author list given at the end of the article.

Published by the American Physical Society under the terms of the [Creative Commons Attribution 3.0 License](https://creativecommons.org/licenses/by/3.0/). Further distribution of this work must maintain attribution to the author(s) and the published article's title, journal citation, and DOI.

TABLE I. Time-dependent functions $h_k(t)$ in Eq. (4).

k	$h_k(t)$
1	$ A_0(t) ^2$
2	$ A_{\parallel}(t) ^2$
3	$ A_{\perp}(t) ^2$
4	$\mathcal{I}m[A_{\parallel}^*(t)A_{\perp}(t)]$
5	$\mathcal{R}e[A_0^*(t)A_{\parallel}(t)]$
6	$\mathcal{I}m[A_0^*(t)A_{\perp}(t)]$
7	$ A_S(t) ^2$
8	$\mathcal{R}e[A_S^*(t)A_{\parallel}(t)]$
9	$\mathcal{I}m[A_S^*(t)A_{\perp}(t)]$
10	$\mathcal{R}e[A_S^*(t)A_0(t)]$

Considering only contributions to first order in z , the decay rate to a CP eigenstate f as a function of the B proper decay time t becomes

$$\begin{aligned} \frac{d\Gamma_f}{dt} \propto e^{-\Gamma t} \{ & [1 + \zeta D_f \mathcal{R}e(z) - S_f \mathcal{I}m(z)] \cosh(\Delta\Gamma t/2) \\ & + [D_f + \mathcal{R}e(z)(C_f + \zeta)] \sinh(\Delta\Gamma t/2) \\ & + \zeta [C_f - D_f \mathcal{R}e(z) + \zeta S_f \mathcal{I}m(z)] \cos(\Delta m t) \\ & - \zeta [S_f - \mathcal{I}m(z)(C_f + \zeta)] \sin(\Delta m t) \}, \end{aligned} \quad (2)$$

where $\Gamma \equiv (\Gamma_{11} + \Gamma_{22})/2$, $\zeta = +1(-1)$ for an initial $|B\rangle$ ($|\bar{B}\rangle$) state and the following definitions are introduced:

$$\begin{aligned} C_f &\equiv \frac{1 - |\lambda_f|^2}{1 + |\lambda_f|^2}, & S_f &\equiv \frac{2\mathcal{I}m(\lambda_f)}{1 + |\lambda_f|^2}, \\ D_f &\equiv -\frac{2\mathcal{R}e(\lambda_f)}{1 + |\lambda_f|^2}, & \lambda_f &\equiv \frac{q\bar{A}_f}{pA_f}, \end{aligned} \quad (3)$$

with A_f and \bar{A}_f being the direct decay amplitudes of a $|B\rangle$ or $|\bar{B}\rangle$ state to the eigenstate f .

For the decay $B^0 \rightarrow J/\psi K_S^0$, the final state is CP odd, corresponding to the CP eigenvalue $\eta_f = -1$. In the SM, $\arg(\lambda_{J/\psi K_S^0}) = \pi - 2\beta$, where β is defined in terms of elements of the CKM matrix as $\beta \equiv \arg[-(V_{cd}V_{cb}^*)/(V_{td}V_{tb}^*)]$. Furthermore, in the B^0 system, the approximation $\Delta\Gamma_d = 0$ is made, as supported by experimental data [20].

The decay $B_s^0 \rightarrow J/\psi K^+ K^-$ is similar to $B^0 \rightarrow J/\psi K_S^0$, but the decay width difference $\Delta\Gamma_s$ cannot be ignored [20]. Another important difference is that the $K^+ K^-$ system mostly originates from the $\phi(1020)$ resonance, giving the $K^+ K^-$ pair an orbital angular momentum $L = 1$ (P wave). Since the $J/\psi\phi$ final state consists of two vector mesons, its orbital angular momentum can be $L \in \{0, 1, 2\}$ for the polarization states $f \in \{0, \perp, \parallel\}$, respectively, with corresponding CP eigenvalues $\eta_f = (-1)^L$. The $K^+ K^-$ system has a small S -wave contribution [18], which results in another $L = 1$ component for the $J/\psi K^+ K^-$ final state. These four polarization states can be separated statistically in the helicity formalism [21], using the three decay angles between the final-state particles. The corresponding weak phases, $\arg(\lambda_{J/\psi K^+ K^-}) = L\pi - \phi_s$, can, in the SM, be expressed in terms of CKM matrix elements, $\phi_s = -2\beta_s \equiv -2\arg[-(V_{ts}V_{tb}^*)/(V_{cs}V_{cb}^*)]$. The decay rate has to be modified compared to Eq. (2) to include the angular dependence. It becomes a sum over all ten combinations of the four helicity amplitudes,

$$\frac{d^4\Gamma_{J/\psi K^+ K^-}}{dt d\vec{\Omega}} \propto \sum_{k=1}^{10} h_k(t) f_k(\vec{\Omega}), \quad (4)$$

where $f_k(\vec{\Omega})$ are angular functions, given in Ref. [21], and $h_k(t)$ are products of the amplitudes as listed in Table I. The time dependence of $h_k(t)$ is given by

$$\begin{aligned} A_l^*(t)A_m(t) &= \frac{A_l^*(0)A_m(0)e^{-\Gamma_s t}}{1 + \zeta C_f} \\ &\times [a_k \cosh(\Delta\Gamma_s t/2) + b_k \sinh(\Delta\Gamma_s t/2) \\ &+ c_k \cos(\Delta m_s t) + d_k \sin(\Delta m_s t)], \end{aligned} \quad (5)$$

with the coefficients listed in Table II.

In the SME, the dimensionless parameter z is not a constant. It depends on the four-velocity $\beta^\mu = (\gamma, \gamma\vec{\beta})$ of the neutral meson as [22,23]

$$z = \frac{\beta^\mu \Delta a_\mu}{\Delta m + i\Delta\Gamma/2}, \quad (6)$$

thereby breaking Lorentz invariance. The SME parameter Δa_μ describes the difference between the couplings of the

TABLE II. Definition of the coefficients in Eq. (5). The following definitions are used: $\eta^+ \equiv (1 + \eta_l \eta_m)/2$, $\eta^- \equiv (1 - \eta_l \eta_m)/2$, $\eta^{\mathcal{I}m} \equiv i(\eta_l - \eta_m)/2$, $\eta^{\mathcal{R}e} \equiv (\eta_l + \eta_m)/2$. Furthermore, $\zeta^+ \equiv (\zeta)^{\eta^+}$, and $\zeta^- \equiv (\zeta)^{\eta^-}$, such that $\zeta^\pm = 1$ if $\eta^\pm = 0$ and $\zeta^\pm = \zeta$ otherwise.

$a_k = (\eta^+ + \eta^- C_f) + \zeta \mathcal{R}e(z)(\eta^{\mathcal{R}e} D_f + \eta^{\mathcal{I}m} S_f) + \mathcal{I}m(z)(\eta^{\mathcal{I}m} D_f - \eta^{\mathcal{R}e} S_f)$
$b_k = (\eta^{\mathcal{R}e} D_f + \eta^{\mathcal{I}m} S_f) + \mathcal{R}e(z)(\zeta^+ + \zeta^- C_f)$
$c_k = \zeta(\eta^- + \eta^+ C_f) - \zeta \mathcal{R}e(z)(\eta^{\mathcal{R}e} D_f + \eta^{\mathcal{I}m} S_f) - \mathcal{I}m(z)(\eta^{\mathcal{I}m} D_f - \eta^{\mathcal{R}e} S_f)$
$d_k = \zeta(\eta^{\mathcal{I}m} D_f - \eta^{\mathcal{R}e} S_f) + \mathcal{I}m(z)(\zeta^+ + \zeta^- C_f)$

valence quarks, within the neutral meson, with the Lorentz-violating fields [22]. Therefore, B^0 and B_s^0 mesons can have different values of Δa_μ . Since Δa_μ is real [24], it follows that $\mathcal{R}e(z)\Delta\Gamma = -2\mathcal{I}m(z)\Delta m$. For B mesons, $\Delta m \gg \Delta\Gamma$, and so $\mathcal{I}m(z)$ is 2 orders of magnitude smaller than $\mathcal{R}e(z)$, and can be ignored in the measurements of Δa_μ . The average boost of B mesons in the acceptance of LHCb is $\langle\gamma\beta\rangle \approx 20$. It follows from Eq. (6) that this large boost results in a high sensitivity to Δa_μ [7].

To measure Δa_μ , the meson direction needs to be determined in an absolute reference frame. Such a frame can be defined with respect to fixed stars [24]. In this frame, the Z axis points north along Earth's rotation axis, the X axis points from the Sun to the vernal equinox on January 1, 2000 (J2000 epoch), and the Y axis completes the right-handed coordinate system. The latitude of the LHCb interaction point is 46.2414°N , the longitude is 6.0963°E , and the angle of the beam east of north is 236.296° . The beam axis is inclined with respect to the geodetic plane by 3.601 mrad , pointing slightly upwards. The timekeeping has been obtained from the LHC machine with a time stamp, t_{LHC} , in UTC microseconds since January 1, 1970, 00:00:00 UTC. The time, spatial coordinates, and angles have negligible uncertainties and are used to define the rotation from the coordinate system of LHCb to the absolute reference frame. For mesons traveling along the beam axis, $\mathcal{R}e(z)$ can be expressed as

$$\begin{aligned}\mathcal{R}e(z) &= \frac{\Delta m}{\Delta m^2 + \Delta\Gamma^2/4} \beta^\mu \Delta a_\mu \\ &\approx \frac{\gamma}{\Delta m} \{ \Delta a_0 + \cos(\chi) \Delta a_Z \\ &\quad + \sin(\chi) [\Delta a_Y \sin(\Omega\hat{t}) + \Delta a_X \cos(\Omega\hat{t})] \}, \quad (7)\end{aligned}$$

where $|\vec{\beta}|$ is set to unity, $\Delta a^{X,Y,Z} = -\Delta a_{X,Y,Z}$, and $\chi = 112.4^\circ$ is the angle between the beam axis and the rotational axis of Earth. The time dependence results from the Earth's rotation, giving a periodicity with sidereal frequency Ω . The sidereal phase at $t_{\text{LHC}} = 0$ is found to be $\hat{t} = (2.8126 \pm 0.0014)\text{ hr}$. The B mesons are emitted at an average angle of about 5° from the beam axis. This means that the LHCb detector is mostly sensitive to the linear combination $\Delta a_\parallel \equiv \Delta a_0 + \cos(\chi) \Delta a_Z = \Delta a_0 - 0.38 \Delta a_Z$, while there is a much weaker sensitivity to the orthogonal parameter, $\Delta a_\perp = 0.38 \Delta a_0 + \Delta a_Z$, coming from the smaller transverse component of the B velocity. Both Δa_\parallel and Δa_\perp are measured and the correlation between them is negligible.

Unbinned likelihood fits are applied to the decay-time distributions using Eqs. (2) and (4). To obtain the SME parameters, the sidereal variation of $\mathcal{R}e(z)$ is taken into account by including in the fits the LHC time and the three-momentum of the reconstructed B candidate. For the B_s^0 sample, the fits are performed to the full angular distribution.

In the invariant mass distributions of the B candidates, the background is mostly combinatorial. For both decay channels, this background is statistically subtracted using the *sPlot* technique [25], which allows us to project out the signal component by weighting each event depending on the mass of the B candidate. The mass models are the same as in Refs. [17,18]. The correlation between the shape of the invariant mass distribution and the B momentum or, for the B_s^0 sample, the decay angles, leads to a small systematic bias for both samples. This effect is included in the systematic uncertainty. In the $B_s^0 \rightarrow J/\psi K^+ K^-$ sample, there is a small contribution coming from misidentified $B^0 \rightarrow J/\psi K^+ \pi^-$ and $\Lambda_b^0 \rightarrow J/\psi p K^-$ decays. This background contribution is statistically removed by adding simulated decays with negative weights. A systematic uncertainty is assigned to account for the uncertainty on the size and shape of this background.

The description of the detection efficiency as a function of the decay time, the decay-time resolution model, and the flavor tagging (to distinguish initial B and \bar{B} mesons) are the same as in Refs. [17] and [18] for the $B^0 \rightarrow J/\psi K_S^0$ and $B_s^0 \rightarrow J/\psi K^+ K^-$ samples, respectively. This description includes the dilution of the asymmetry due to wrong decisions of the flavor tagging method. The decay-time resolution model and tagging calibration do not lead to a systematic bias in the final result. A possible wrong assignment of the primary interaction vertex (PV) to the B candidate gives a small bias in the $\Delta a_\perp^{B^0}$ parameter, which is included in the systematic uncertainty. The inefficiency at high decay times, caused by the reconstruction algorithms, is described by an exponential function. For the B^0 sample, this function is obtained from simulation and does not lead to a systematic bias in the result. For the B_s^0 sample, the exponential function is obtained from a data-driven method. The change in the final result when using the correction procedure from Ref. [18] is taken as a systematic uncertainty.

The production asymmetry between B^0 and \bar{B}^0 mesons is included in the modeling of the decay rates, and is taken from Refs. [26,27]. The corresponding uncertainties are included in the statistical uncertainty, while a possible momentum dependence of the production asymmetry is considered as a systematic uncertainty. The B_s^0 production asymmetry does not affect the fit to the B_s^0 sample, since the fast B_s^0 oscillations wash out this effect and the decay rates for B_s^0 and \bar{B}_s^0 tags are normalized separately.

In the fit to the B^0 sample, the correlation between $\mathcal{R}e(z^{B^0})$ and $C_{J/\psi K_S^0}$ is too large to allow determination of $\mathcal{R}e(z^{B^0})$ without making assumptions about the value of $C_{J/\psi K_S^0}$ [7]. On the other hand, to determine $\Delta a_\mu^{B^0}$, the averages $C_{J/\psi K_S^0} = 0.005 \pm 0.020$ and $S_{J/\psi K_S^0} = 0.676 \pm 0.021$ [19] as measured by the BABAR and Belle collaborations can be used in the fit. Since the boost

of the B^0 mesons is about 40 times lower in these experiments, these values are hardly affected by possible Lorentz violation in the SME. The value of $D_{J/\psi K_S^0}$ is by definition $\sqrt{1 - S_{J/\psi K_S^0}^2 - C_{J/\psi K_S^0}^2}$. The uncertainties on these external input values are propagated as systematic uncertainties on $\Delta a_\mu^{B^0}$. The mass difference, $\Delta m_d = 0.510 \pm 0.003 \text{ ps}^{-1}$ [19], is allowed to vary in the fit within its uncertainty using a Gaussian constraint. Setting $\Delta\Gamma_d = 0.007 \text{ ps}^{-1}$, which corresponds to the experimental uncertainty [20], leads to a small change in $\Delta a_\mu^{B^0}$, which is included in the systematic uncertainty. The B^0 lifetime is allowed to vary freely in the fit.

In the fit to the B_s^0 sample, the correlation between $\text{Re}(z^{B_s^0})$ and $C_{J/\psi K^+ K^-}$ is small owing to the additional interference terms from the helicity amplitudes, the nonzero $\Delta\Gamma_s$, and the faster B_s^0 - \bar{B}_s^0 oscillations. For this reason, the same parameters as in Ref. [18] are varied freely in the fit, in addition to either Δa_μ or z . The detection efficiency is also described as a function of the decay angles. The shape of this angular acceptance is obtained from simulation. The simulated events are weighted to match the kinematic distributions in data. The uncertainty due to the limited number of simulated events and the full effect of correcting for the kinematic distributions in data are added to the systematic uncertainty. Systematic effects due to the decay-angle resolution are negligibly small. The fit to the B_s^0 sample is performed simultaneously in bins of the $K^+ K^-$ invariant mass [18]. Each bin has a different interference between the P - and S -wave amplitudes. This effect is included in the fit and no systematic biases are observed.

An overview of the systematic uncertainties is given in Table III. For the B^0 mixing, the largest contribution comes from the uncertainty on the external parameters C_f and S_f . A small systematic bias is observed in $\Delta a_\mu^{B^0}$ due to the momentum dependence of the cross sections of neutral kaons in the detector material. For the B_s^0 mixing, the largest contribution comes from the description of the decay-time acceptance. Effects from the correlation between the mass and decay time and from the accuracy of the length scale and momentum scale of the detector are found to be negligible.

The components of the SME parameter Δa_μ for B^0 mixing, obtained from the fit to the sample of selected $B^0 \rightarrow J/\psi K_S^0$ candidates, are

$$\begin{aligned}\Delta a_\parallel^{B^0} &= [-0.10 \pm 0.82(\text{stat}) \pm 0.54(\text{syst})] \times 10^{-15} \text{ GeV}, \\ \Delta a_\perp^{B^0} &= [-0.20 \pm 0.22(\text{stat}) \pm 0.04(\text{syst})] \times 10^{-13} \text{ GeV}, \\ \Delta a_X^{B^0} &= [+1.97 \pm 1.30(\text{stat}) \pm 0.29(\text{syst})] \times 10^{-15} \text{ GeV}, \\ \Delta a_Y^{B^0} &= [+0.44 \pm 1.26(\text{stat}) \pm 0.29(\text{syst})] \times 10^{-15} \text{ GeV},\end{aligned}$$

and the corresponding numbers for B_s^0 mixing, using $B_s^0 \rightarrow J/\psi K^+ K^-$ candidates, are

TABLE III. Systematic uncertainties on Δa_μ for B^0 mixing and on Δa_μ and z for B_s^0 mixing. Contributions marked with centered dots are negligible.

B^0 mixing	Δa_\parallel	Δa_\perp	$\Delta a_{X,Y}$
Source	[$\times 10^{-15}$ GeV]		
Mass correlation	0.04
Wrong PV assignment	...	1	...
Production asymmetry	0.28	1	0.05
External input C_f, S_f	0.46	4	0.28
Decay width difference	0.07
Neutral kaon asymmetry	...	1	...
Quadratic sum	0.54	4	0.29

B_s^0 mixing	Δa_\parallel	Δa_\perp	$\Delta a_{X,Y}$	$\text{Re}(z)$	$\text{Im}(z)$
Source	[$\times 10^{-14}$ GeV]				
Mass correlation	0.10	3	0.24	0.001	0.002
Peaking background	0.14	3	0.15	0.003	...
Decay-time acceptance	0.30	7	0.65	...	0.001
Angular acceptance	0.07	0.002	0.001
Quadratic sum	0.36	8	0.71	0.003	0.002

$$\begin{aligned}\Delta a_\parallel^{B_s^0} &= [-0.89 \pm 1.41(\text{stat}) \pm 0.36(\text{syst})] \times 10^{-14} \text{ GeV}, \\ \Delta a_\perp^{B_s^0} &= [-0.47 \pm 0.39(\text{stat}) \pm 0.08(\text{syst})] \times 10^{-12} \text{ GeV}, \\ \Delta a_X^{B_s^0} &= [+1.01 \pm 2.08(\text{stat}) \pm 0.71(\text{syst})] \times 10^{-14} \text{ GeV}, \\ \Delta a_Y^{B_s^0} &= [-3.83 \pm 2.09(\text{stat}) \pm 0.71(\text{syst})] \times 10^{-14} \text{ GeV}.\end{aligned}$$

Figure 1 shows the result of fits of $\text{Re}(z)$ in bins of the sidereal phase for both samples. For the B^0 sample, the external constraints on $C_{J/\psi K_S^0}$ and $S_{J/\psi K_S^0}$ are again used. No sidereal variation is observed. Independently of any

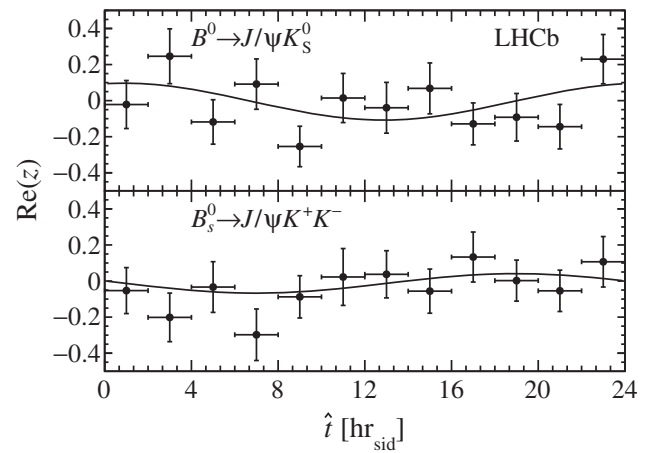


FIG. 1. Values of $\text{Re}(z)$ obtained from fits in bins of sidereal phase for (top) the B^0 sample and (bottom) the B_s^0 sample. The solid line shows the variation of $\text{Re}(z)$ from the Δa_μ fits, using the average B momentum.

assumption of Lorentz violation, the complex CPT -violating parameter z in the B_s^0 system is found to be

$$\text{Re}(z^{B_s^0}) = -0.022 \pm 0.033(\text{stat}) \pm 0.003(\text{syst}),$$

$$\text{Im}(z^{B_s^0}) = 0.004 \pm 0.011(\text{stat}) \pm 0.002(\text{syst}).$$

Since the SME fits consider only one specific frequency, i.e., the sidereal frequency, a wide range of frequencies is scanned by means of the periodogram method. A periodogram gives the spectral power $P(\nu)$ of a frequency ν in a signal sampled at discrete, not necessarily equidistant, times. In this analysis, the Lomb-Scargle periodogram [28] is used, as in the $BABAR$ measurement of $\Delta a_\mu^{B^0}$ [8].

The periodogram is determined for the term in the decay rates proportional to $e^{-\Gamma t} \text{Re}(z)$. Since negative weights cannot be used in the periodogram, the B mass windows are narrowed to $5260 < m_{J/\psi K_S^0} < 5300 \text{ MeV}/c^2$ and $5350 < m_{J/\psi K^+ K^-} < 5390 \text{ MeV}/c^2$ compared to those used in the fits [17,18]. In total about 5200 frequencies are scanned in a wide range around the sidereal frequency, from 0.03 to 2.10 solar day $^{-1}$. The number of frequencies oversamples the number of independent frequencies by roughly a factor of 2, thereby avoiding any undersampling [29]. As the data are unevenly sampled, the false-alarm probability is determined from simulation [29], where the time stamps are taken from data.

The two periodograms are shown in Fig. 2. No significant peaks are found. For the B^0 periodogram, the highest peak $P(\nu_{\text{max}}) = 8.09$ is found at a frequency of 1.5507 solar day $^{-1}$ and has a false-alarm probability of 0.57. There are 2707 (1559) sampled frequencies with a larger spectral power than the peak at the sidereal (solar) frequency. For the B_s^0

periodogram the highest peak $P(\nu_{\text{max}}) = 10.85$ is found at a frequency of 1.3301 solar day $^{-1}$ and has a false-alarm probability of 0.06. There are 3386 (2356) frequencies with a larger spectral power than the sidereal (solar) peak. The absence of any signal in the SME fits is confirmed by the absence of significant peaks at the sidereal frequency.

The results presented here are consistent with CPT symmetry and Lorentz invariance. The measurement of $\Delta a_\mu^{B^0}$ is an improvement in precision of about 3 orders of magnitude compared to the one from the $BABAR$ collaboration [8] when the SM prediction $\Delta \Gamma_d = -0.0027 \text{ ps}^{-1}$ [30] is used to scale their result. The measurement of $\Delta a_\mu^{B_s^0}$ is an order of magnitude more precise than the one from the D0 collaboration [9] (note the different definition, $\Delta a_\perp \equiv \sqrt{\Delta a_X^2 + \Delta a_Y^2}$, in Ref. [9]). The measurement of $z^{B_s^0}$ is the first direct measurement of this quantity.

We express our gratitude to our colleagues in the CERN accelerator departments for the excellent performance of the LHC. We thank the technical and administrative staff at the LHCb institutes. We acknowledge support from CERN and from the following national agencies: CAPES, CNPq, FAPERJ, and FINEP (Brazil); NSFC (China); CNRS/IN2P3 (France); BMBF, DFG, and MPG (Germany); INFN (Italy); FOM and NWO (Netherlands); MNiSW and NCN (Poland); MEN/IFA (Romania); MinES and FANO (Russia); MinEco (Spain); SNSF and SER (Switzerland); NASU (Ukraine); STFC (United Kingdom); and NSF (USA). We acknowledge the computing resources that are provided by CERN, IN2P3 (France); KIT and DESY (Germany); INFN (Italy); SURF (Netherlands), PIC (Spain); GridPP (United Kingdom); RRCKI and Yandex LLC (Russia); CSCS (Switzerland); IFIN-HH (Romania); CBPF (Brazil); PL-GRID (Poland); and OSC (USA). We are indebted to the communities behind the multiple open source software packages on which we depend. Individual groups or members have received support from AvH Foundation (Germany); EPLANET; Marie Skłodowska-Curie Actions and ERC (European Union); Conseil Général de Haute-Savoie; Labex ENIGMASS and OCEVU; Région Auvergne (France); RFBR and Yandex LLC (Russia); GVA, XuntaGal, and GENCAT (Spain); Herchel Smith Fund; the Royal Society, Royal Commission for the Exhibition of 1851, and the Leverhulme Trust (United Kingdom).

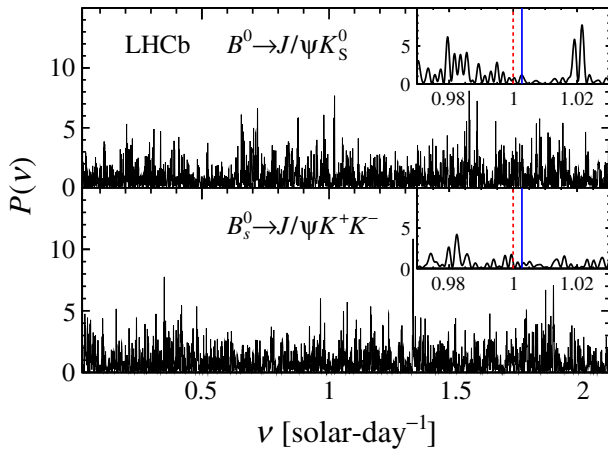


FIG. 2. Periodograms for (top) the B^0 and (bottom) B_s^0 sample. The insets show a zoom around the solar (red dashed line) and sidereal (blue solid line) frequencies, which have been made by highly oversampling the frequencies in this narrow range.

- [1] O. W. Greenberg, *Phys. Rev. Lett.* **89**, 231602 (2002).
- [2] V. A. Kostelecký and S. Samuel, *Phys. Rev. D* **39**, 683 (1989).
- [3] S. Liberati, *Classical Quantum Gravity* **30**, 133001 (2013).
- [4] D. Colladay and V. A. Kostelecký, *Phys. Rev. D* **55**, 6760 (1997).
- [5] D. Colladay and V. A. Kostelecký, *Phys. Rev. D* **58**, 116002 (1998).

- [6] V. A. Kostelevy and R. Potting, *Nucl. Phys.* **B359**, 545 (1991); V. A. Kostelevy and R. Potting, *Phys. Rev. D* **51**, 3923 (1995).
- [7] J. van Tilburg and M. van Veghel, *Phys. Lett. B* **742**, 236 (2015).
- [8] B. Aubert *et al.* (BABAR Collaboration), *Phys. Rev. Lett.* **100**, 131802 (2008).
- [9] V. M. Abazov *et al.* (D0 Collaboration), *Phys. Rev. Lett.* **115**, 161601 (2015); V. M. Abazov *et al.* (D0 Collaboration), *Phys. Rev. Lett.* **116**, 019901 (2016).
- [10] A. A. Alves, Jr. *et al.* (LHCb Collaboration), *J. Instrum.* **3**, S08005 (2008).
- [11] R. Aaij *et al.* (LHCb Collaboration), *Int. J. Mod. Phys. A* **30**, 1530022 (2015).
- [12] T. Sjöstrand, S. Mrenna, and P. Skands, *J. High Energy Phys.* **05** (2006) 026; T. Sjöstrand, S. Mrenna, and P. Skands, *Comput. Phys. Commun.* **178**, 852 (2008).
- [13] I. Belyaev *et al.*, *J. Phys. Conf. Ser.* **331**, 032047 (2011).
- [14] D. J. Lange, *Nucl. Instrum. Methods Phys. Res., Sect. A* **462**, 152 (2001).
- [15] J. Allison, K. Amako, J. Apostolakis, H. Araujo, P. Dubois *et al.* (Geant4 Collaboration), *IEEE Trans. Nucl. Sci.* **53**, 270 (2006); S. Agostinelli *et al.* (Geant4 Collaboration), *Nucl. Instrum. Methods Phys. Res., Sect. A* **506**, 250 (2003).
- [16] M. Clemencic, G. Corti, S. Easo, C. R. Jones, S. Miglioranza, M. Pappagallo, and P. Robbe, *J. Phys. Conf. Ser.* **331**, 032023 (2011).
- [17] R. Aaij *et al.* (LHCb Collaboration), *Phys. Rev. Lett.* **115**, 031601 (2015).
- [18] R. Aaij *et al.* (LHCb Collaboration), *Phys. Rev. Lett.* **114**, 041801 (2015).
- [19] K. A. Olive *et al.* (Particle Data Group), *Chin. Phys.* **C38**, 090001 (2014).
- [20] Y. Amhis *et al.* (Heavy Flavor Averaging Group), *arXiv*: 1412.7515.
- [21] R. Aaij *et al.* (LHCb Collaboration), *Phys. Rev. D* **87**, 112010 (2013).
- [22] V. A. Kostelevy, *Phys. Rev. Lett.* **80**, 1818 (1998).
- [23] V. A. Kostelevy, *Phys. Rev. D* **64**, 076001 (2001).
- [24] V. A. Kostelevy, *Phys. Rev. D* **61**, 016002 (1999).
- [25] M. Pivk and F. R. Le Diberder, *Nucl. Instrum. Methods Phys. Res., Sect. A* **555**, 356 (2005).
- [26] R. Aaij *et al.* (LHCb Collaboration), *Phys. Lett. B* **739**, 218 (2014).
- [27] R. Aaij *et al.* (LHCb Collaboration), *Phys. Rev. Lett.* **114**, 041601 (2015).
- [28] J. Scargle, *Astrophys. J.* **263**, 835 (1982).
- [29] J. Horne and S. Baliunas, *Astrophys. J.* **302**, 757 (1986).
- [30] A. Lenz and U. Nierste, *J. High Energy Phys.* **06** (2007) 072.

R. Aaij,³⁹ C. Abellán Beteta,⁴¹ B. Adeva,³⁸ M. Adinolfi,⁴⁷ Z. Ajaltouni,⁵ S. Akar,⁶ J. Albrecht,¹⁰ F. Alessio,³⁹ M. Alexander,⁵² S. Ali,⁴² G. Alkhazov,³¹ P. Alvarez Cartelle,⁵⁴ A. A. Alves Jr.,⁵⁸ S. Amato,² S. Amerio,²³ Y. Amhis,⁷ L. An,^{3,40} L. Anderlini,¹⁸ G. Andreassi,⁴⁰ M. Andreotti,^{17,a} J. E. Andrews,⁵⁹ R. B. Appleby,⁵⁵ O. Aquines Gutierrez,¹¹ F. Archilli,³⁹ P. d'Argent,¹² A. Artamonov,³⁶ M. Artuso,⁶⁰ E. Aslanides,⁶ G. Auriemma,^{26,b} M. Baalouch,⁵ S. Bachmann,¹² J. J. Back,⁴⁹ A. Badalov,³⁷ C. Baesso,⁶¹ S. Baker,⁵⁴ W. Baldini,¹⁷ R. J. Barlow,⁵⁵ C. Barschel,³⁹ S. Barsuk,⁷ W. Barter,³⁹ V. Batozskaya,²⁹ V. Battista,⁴⁰ A. Bay,⁴⁰ L. Beaucourt,⁴ J. Beddow,⁵² F. Bedeschi,²⁴ I. Bediaga,¹ L. J. Bel,⁴² V. Bellec,⁴⁰ N. Belloli,^{21,c} I. Belyaev,³² E. Ben-Haim,⁸ G. Bencivenni,¹⁹ S. Benson,³⁹ J. Benton,⁴⁷ A. Berezhnoy,³³ R. Bernet,⁴¹ A. Bertolin,²³ F. Betti,¹⁵ M.-O. Bettler,³⁹ M. van Beuzekom,⁴² S. Bifani,⁴⁶ P. Billoir,⁸ T. Bird,⁵⁵ A. Birnkraut,¹⁰ A. Bizzeti,^{18,d} T. Blake,⁴⁹ F. Blanc,⁴⁰ J. Blouw,¹¹ S. Blusk,⁶⁰ V. Bocci,²⁶ A. Bondar,³⁵ N. Bondar,^{31,39} W. Bonivento,¹⁶ A. Borgheresi,^{21,c} S. Borghi,⁵⁵ M. Borisyak,⁶⁷ M. Borsato,³⁸ M. Boubdir,⁹ T. J. V. Bowcock,⁵³ E. Bowen,⁴¹ C. Bozzi,^{17,39} S. Braun,¹² M. Britsch,¹² T. Britton,⁶⁰ J. Brodzicka,⁵⁵ E. Buchanan,⁴⁷ C. Burr,⁵⁵ A. Bursche,² J. Buytaert,³⁹ S. Cadeddu,¹⁶ R. Calabrese,^{17,a} M. Calvi,^{21,c} M. Calvo Gomez,^{37,e} P. Campana,¹⁹ D. Campora Perez,³⁹ L. Capriotti,⁵⁵ A. Carbone,^{15,f} G. Carboni,^{25,g} R. Cardinale,^{20,h} A. Cardini,¹⁶ P. Carniti,^{21,c} L. Carson,⁵¹ K. Carvalho Akiba,² G. Casse,⁵³ L. Cassina,^{21,c} L. Castillo Garcia,⁴⁰ M. Cattaneo,³⁹ Ch. Cauet,¹⁰ G. Cavallero,²⁰ R. Cenci,^{24,i} M. Charles,⁸ Ph. Charpentier,³⁹ G. Chatzikonstantinidis,⁴⁶ M. Chefdeville,⁴ S. Chen,⁵⁵ S.-F. Cheung,⁵⁶ M. Chrzasczcz,^{41,27} X. Cid Vidal,³⁹ G. Ciezarek,⁴² P. E. L. Clarke,⁵¹ M. Clemencic,³⁹ H. V. Cliff,⁴⁸ J. Closier,³⁹ V. Coco,⁵⁸ J. Cogan,⁶ E. Cogneras,⁵ V. Cogoni,^{16,j} L. Cojocariu,³⁰ G. Collazuol,^{23,k} P. Collins,³⁹ A. Comerma-Montells,¹² A. Contu,³⁹ A. Cook,⁴⁷ M. Coombes,⁴⁷ S. Coquereau,⁸ G. Corti,³⁹ M. Corvo,^{17,a} B. Couturier,³⁹ G. A. Cowan,⁵¹ D. C. Craik,⁵¹ A. Crocombe,⁴⁹ M. Cruz Torres,⁶¹ S. Cunliffe,⁵⁴ R. Currie,⁵⁴ C. D'Ambrosio,³⁹ E. Dall'Occo,⁴² J. Dalseno,⁴⁷ P. N. Y. David,⁴² A. Davis,⁵⁸ O. De Aguiar Francisco,² K. De Bruyn,⁶ S. De Capua,⁵⁵ M. De Cian,¹² J. M. De Miranda,¹ L. De Paula,² P. De Simone,¹⁹ C.-T. Dean,⁵² D. Decamp,⁴ M. Deckenhoff,¹⁰ L. Del Buono,⁸ N. Déleage,⁴ M. Demmer,¹⁰ D. Derkach,⁶⁷ O. Deschamps,⁵ F. Dettori,³⁹ B. Dey,²² A. Di Canto,³⁹ F. Di Ruscio,²⁵ H. Dijkstra,³⁹ F. Dordei,³⁹ M. Dorigo,⁴⁰ A. Dosil Suárez,³⁸ A. Dovbnya,⁴⁴ K. Dreimanis,⁵³ L. Dufour,⁴² G. Dujany,⁵⁵ K. Dungs,³⁹ P. Durante,³⁹ R. Dzhelezhadine,³⁶ A. Dziurda,²⁷ A. Dzyuba,³¹ S. Easo,^{50,39} U. Egede,⁵⁴ V. Egorychev,³² S. Eidelman,³⁵ S. Eisenhardt,⁵¹ U. Eitschberger,¹⁰ R. Ekelhof,¹⁰ L. Eklund,⁵² I. El Rifai,⁵ Ch. Elsasser,⁴¹ S. Ely,⁶⁰ S. Esen,¹² H. M. Evans,⁴⁸ T. Evans,⁵⁶ A. Falabella,¹⁵ C. Färber,³⁹

- N. Farley,⁴⁶ S. Farry,⁵³ R. Fay,⁵³ D. Fazzini,^{21,c} D. Ferguson,⁵¹ V. Fernandez Albor,³⁸ F. Ferrari,¹⁵ F. Ferreira Rodrigues,¹ M. Ferro-Luzzi,³⁹ S. Filippov,³⁴ M. Fiore,^{17,a} M. Fiorini,^{17,a} M. Firlej,²⁸ C. Fitzpatrick,⁴⁰ T. Fiutowski,²⁸ F. Fleuret,^{7,1} K. Fohl,³⁹ M. Fontana,¹⁶ F. Fontanelli,^{20,h} D. C. Forshaw,⁶⁰ R. Forty,³⁹ M. Frank,³⁹ C. Frei,³⁹ M. Frosini,¹⁸ J. Fu,²² E. Furfaro,^{25,g} A. Gallas Torreira,³⁸ D. Galli,^{15,f} S. Gallorini,²³ S. Gambetta,⁵¹ M. Gandelman,² P. Gandini,⁵⁶ Y. Gao,³ J. García Pardiñas,³⁸ J. Garra Tico,⁴⁸ L. Garrido,³⁷ P. J. Garsed,⁴⁸ D. Gascon,³⁷ C. Gaspar,³⁹ L. Gavardi,¹⁰ G. Gazzoni,⁵ D. Gerick,¹² E. Gersabeck,¹² M. Gersabeck,⁵⁵ T. Gershon,⁴⁹ Ph. Ghez,⁴ S. Gianì,⁴⁰ V. Gibson,⁴⁸ O. G. Girard,⁴⁰ L. Giubega,³⁰ V. V. Gligorov,³⁹ C. Göbel,⁶¹ D. Golubkov,³² A. Golutvin,^{54,39} A. Gomes,^{1,m} C. Gotti,^{21,c} M. Grabalosa Gándara,⁵ R. Graciani Diaz,³⁷ L. A. Granado Cardoso,³⁹ E. Graugés,³⁷ E. Graverini,⁴¹ G. Graziani,¹⁸ A. Grecu,³⁰ P. Griffith,⁴⁶ L. Grillo,¹² O. Grünberg,⁶⁵ E. Gushchin,³⁴ Yu. Guz,^{36,39} T. Gys,³⁹ T. Hadavizadeh,⁵⁶ C. Hadjivasiliou,⁶⁰ G. Haefeli,⁴⁰ C. Haen,³⁹ S. C. Haines,⁴⁸ S. Hall,⁵⁴ B. Hamilton,⁵⁹ X. Han,¹² S. Hansmann-Menzemer,¹² N. Harnew,⁵⁶ S. T. Harnew,⁴⁷ J. Harrison,⁵⁵ J. He,³⁹ T. Head,⁴⁰ A. Heister,⁹ K. Hennessy,⁵³ P. Henrard,⁵ L. Henry,⁸ J. A. Hernando Morata,³⁸ E. van Herwijnen,³⁹ M. Heß,⁶⁵ A. Hicheur,² D. Hill,⁵⁶ M. Hoballah,⁵ C. Hombach,⁵⁵ L. Hongming,⁴⁰ W. Hulsbergen,⁴² T. Humair,⁵⁴ M. Hushchyn,⁶⁷ N. Hussain,⁵⁶ D. Hutchcroft,⁵³ M. Idzik,²⁸ P. Ilten,⁵⁷ R. Jacobsson,³⁹ A. Jaeger,¹² J. Jalocha,⁵⁶ E. Jans,⁴² A. Jawahery,⁵⁹ M. John,⁵⁶ D. Johnson,³⁹ C. R. Jones,⁴⁸ C. Joram,³⁹ B. Jost,³⁹ N. Jurik,⁶⁰ S. Kandybei,⁴⁴ W. Kalso,⁶ M. Karacson,³⁹ T. M. Karbach,³⁹ S. Karodia,⁵² M. Kecke,¹² M. Kelsey,⁶⁰ I. R. Kenyon,⁴⁶ M. Kenzie,³⁹ T. Ketel,⁴³ E. Khairullin,⁶⁷ B. Khanji,^{21,39,c} C. Khurewathanakul,⁴⁰ T. Kirm,⁹ S. Klaver,⁵⁵ K. Klimaszewski,²⁹ M. Kolpin,¹² I. Komarov,⁴⁰ R. F. Koopman,⁴³ P. Koppenburg,^{42,39} M. Kozeiha,⁵ L. Kravchuk,³⁴ K. Kreplin,¹² M. Kreps,⁴⁹ P. Krokovny,³⁵ F. Kruse,¹⁰ W. Krzemien,²⁹ W. Kucewicz,^{27,n} M. Kucharczyk,²⁷ V. Kudryavtsev,³⁵ A. K. Kuonen,⁴⁰ K. Kurek,²⁹ T. Kvaratskheliya,³² D. Lacarrere,³⁹ G. Lafferty,^{55,39} A. Lai,¹⁶ D. Lambert,⁵¹ G. Lanfranchi,¹⁹ C. Langenbruch,⁴⁹ B. Langhans,³⁹ T. Latham,⁴⁹ C. Lazzeroni,⁴⁶ R. Le Gac,⁶ J. van Leerdam,⁴² J.-P. Lees,⁴ R. Lefèvre,⁵ A. Leflat,^{33,39} J. Lefrançois,⁷ E. Lemos Cid,³⁸ O. Leroy,⁶ T. Lesiak,²⁷ B. Leverington,¹² Y. Li,⁷ T. Likhomanenko,^{67,66} R. Lindner,³⁹ C. Linn,³⁹ F. Lionetto,⁴¹ B. Liu,¹⁶ X. Liu,³ D. Loh,⁴⁹ I. Longstaff,⁵² J. H. Lopes,² D. Lucchesi,^{23,k} M. Lucio Martinez,³⁸ H. Luo,⁵¹ A. Lupato,²³ E. Luppi,^{17,a} O. Lupton,⁵⁶ N. Lusardi,²² A. Lusiani,²⁴ X. Lyu,⁶² F. Machefert,⁷ F. Maciuc,³⁰ O. Maev,³¹ K. Maguire,⁵⁵ S. Malde,⁵⁶ A. Malinin,⁶⁶ G. Manca,⁷ G. Mancinelli,⁶ P. Manning,⁶⁰ A. Mapelli,³⁹ J. Maratas,⁵ J. F. Marchand,⁴ U. Marconi,¹⁵ C. Marin Benito,³⁷ P. Marino,^{24,i} J. Marks,¹² G. Martellotti,²⁶ M. Martin,⁶ M. Martinelli,⁴⁰ D. Martinez Santos,³⁸ F. Martinez Vidal,⁶⁸ D. Martins Tostes,² L. M. Massacrier,⁷ A. Massafferri,¹ R. Matev,³⁹ A. Mathad,⁴⁹ Z. Mathe,³⁹ C. Matteuzzi,²¹ A. Mauri,⁴¹ B. Maurin,⁴⁰ A. Mazurov,⁴⁶ M. McCann,⁵⁴ J. McCarthy,⁴⁶ A. McNab,⁵⁵ R. McNulty,¹³ B. Meadows,⁵⁸ F. Meier,¹⁰ M. Meissner,¹² D. Melnychuk,²⁹ M. Merk,⁴² A. Merli,^{22,o} E. Michielin,²³ D. A. Milanes,⁶⁴ M.-N. Minard,⁴ D. S. Mitzel,¹² J. Molina Rodriguez,⁶¹ I. A. Monroy,⁶⁴ S. Monteil,⁵ M. Morandin,²³ P. Morawski,²⁸ A. Mordà,⁶ M. J. Morello,^{24,i} J. Moron,²⁸ A. B. Morris,⁵¹ R. Mountain,⁶⁰ F. Muheim,⁵¹ D. Müller,⁵⁵ J. Müller,¹⁰ K. Müller,⁴¹ V. Müller,¹⁰ M. Mussini,¹⁵ B. Muster,⁴⁰ P. Naik,⁴⁷ T. Nakada,⁴⁰ R. Nandakumar,⁵⁰ A. Nandi,⁵⁶ I. Nasteva,² M. Needham,⁵¹ N. Neri,²² S. Neubert,¹² N. Neufeld,³⁹ M. Neuner,¹² A. D. Nguyen,⁴⁰ C. Nguyen-Mau,^{40,p} V. Niess,⁵ S. Nieswand,⁹ R. Niet,¹⁰ N. Nikitin,³³ T. Nikodem,¹² A. Novoselov,³⁶ D. P. O'Hanlon,⁴⁹ A. Oblakowska-Mucha,²⁸ V. Obraztsov,³⁶ S. Ogilvy,⁵² O. Okhrimenko,⁴⁵ R. Oldeman,^{16,48,j} C. J. G. Onderwater,⁶⁹ B. Osorio Rodrigues,¹ J. M. Otalora Goicochea,² A. Otto,³⁹ P. Owen,⁵⁴ A. Oyanguren,⁶⁸ A. Palano,^{14,q} F. Palombo,^{22,o} M. Palutan,¹⁹ J. Panman,³⁹ A. Papanestis,⁵⁰ M. Pappagallo,⁵² L. L. Pappalardo,^{17,a} C. Pappenheimer,⁵⁸ W. Parker,⁵⁹ C. Parkes,⁵⁵ G. Passaleva,¹⁸ G. D. Patel,⁵³ M. Patel,⁵⁴ C. Patrignani,^{20,h} A. Pearce,^{55,50} A. Pellegrino,⁴² G. Penso,^{26,r} M. Pepe Altarelli,³⁹ S. Perazzini,^{15,f} P. Perret,⁵ L. Pescatore,⁴⁶ K. Petridis,⁴⁷ A. Petrolini,^{20,h} M. Petruzzo,²² E. Picatoste Olloqui,³⁷ B. Pietrzyk,⁴ M. Pikies,²⁷ D. Pinci,²⁶ A. Pistone,²⁰ A. Piucci,¹² S. Playfer,⁵¹ M. Plo Casasus,³⁸ T. Poikela,³⁹ F. Polci,⁸ A. Poluektov,^{49,35} I. Polyakov,³² E. Polcarpo,² A. Popov,³⁶ D. Popov,^{11,39} B. Popovici,³⁰ C. Potterat,² E. Price,⁴⁷ J. D. Price,⁵³ J. Prisciandaro,³⁸ A. Pritchard,⁵³ C. Prouve,⁴⁷ V. Pugatch,⁴⁵ A. Puig Navarro,⁴⁰ G. Punzi,^{24,s} W. Qian,⁵⁶ R. Quagliani,^{7,47} B. Rachwal,²⁷ J. H. Rademacker,⁴⁷ M. Rama,²⁴ M. Ramos Pernas,³⁸ M. S. Rangel,² I. Raniuk,⁴⁴ G. Raven,⁴³ F. Redi,⁵⁴ S. Reichert,⁵⁵ A. C. dos Reis,¹ V. Renaudin,⁷ S. Ricciardi,⁵⁰ S. Richards,⁴⁷ M. Rihl,³⁹ K. Rinnert,^{53,39} V. Rives Molina,³⁷ P. Robbe,⁷ A. B. Rodrigues,¹ E. Rodrigues,⁵⁵ J. A. Rodriguez Lopez,⁶⁴ P. Rodriguez Perez,⁵⁵ A. Rogozhnikov,⁶⁷ S. Roiser,³⁹ V. Romanovsky,³⁶ A. Romero Vidal,³⁸ J. W. Ronayne,¹³ M. Rotondo,²³ T. Ruf,³⁹ P. Ruiz Valls,⁶⁸ J. J. Saborido Silva,³⁸ N. Sagidova,³¹ B. Saitta,^{16,j} V. Salustino Guimaraes,² C. Sanchez Mayordomo,⁶⁸ B. Sanmartin Sedes,³⁸ R. Santacesaria,²⁶ C. Santamarina Rios,³⁸ M. Santimaria,¹⁹ E. Santovetti,^{25,g} A. Sarti,^{19,r} C. Satriano,^{26,b} A. Satta,²⁵ D. M. Saunders,⁴⁷ D. Savrina,^{32,33} S. Schael,⁹ M. Schiller,³⁹ H. Schindler,³⁹ M. Schlupp,¹⁰ M. Schmelling,¹¹ T. Schmelzer,¹⁰ B. Schmidt,³⁹ O. Schneider,⁴⁰ A. Schopper,³⁹ M. Schubiger,⁴⁰ M.-H. Schune,⁷

R. Schwemmer,³⁹ B. Sciascia,¹⁹ A. Sciubba,^{26,r} A. Semennikov,³² A. Sergi,⁴⁶ N. Serra,⁴¹ J. Serrano,⁶ L. Sestini,²³ P. Seyfert,²¹ M. Shapkin,³⁶ I. Shapoval,^{17,44,a} Y. Shcheglov,³¹ T. Shears,⁵³ L. Shekhtman,³⁵ V. Shevchenko,⁶⁶ A. Shires,¹⁰ B. G. Siddi,¹⁷ R. Silva Coutinho,⁴¹ L. Silva de Oliveira,² G. Simi,^{23,s} M. Sirendi,⁴⁸ N. Skidmore,⁴⁷ T. Skwarnicki,⁶⁰ E. Smith,⁵⁴ I. T. Smith,⁵¹ J. Smith,⁴⁸ M. Smith,⁵⁵ H. Snoek,⁴² M. D. Sokoloff,⁵⁸ F. J. P. Soler,⁵² F. Soomro,⁴⁰ D. Souza,⁴⁷ B. Souza De Paula,² B. Spaan,¹⁰ P. Spradlin,⁵² S. Sridharan,³⁹ F. Stagni,³⁹ M. Stahl,¹² S. Stahl,³⁹ S. Stefkova,⁵⁴ O. Steinkamp,⁴¹ O. Stenyakin,³⁶ S. Stevenson,⁵⁶ S. Stoica,³⁰ S. Stone,⁶⁰ B. Storaci,⁴¹ S. Stracka,^{24,i} M. Straticiuc,³⁰ U. Straumann,⁴¹ L. Sun,⁵⁸ W. Sutcliffe,⁵⁴ K. Swientek,²⁸ S. Swientek,¹⁰ V. Syropoulos,⁴³ M. Szczekowski,²⁹ T. Szumlak,²⁸ S. T'Jampens,⁴ A. Tayduganov,⁶ T. Tekampe,¹⁰ G. Tellarini,^{17,a} F. Teubert,³⁹ C. Thomas,⁵⁶ E. Thomas,³⁹ J. van Tilburg,⁴² V. Tisserand,⁴ M. Tobin,⁴⁰ S. Tolk,⁴³ L. Tomassetti,^{17,a} D. Tonelli,³⁹ S. Topp-Joergensen,⁵⁶ E. Tournefier,⁴ S. Tourneur,⁴⁰ K. Trabelsi,⁴⁰ M. Traill,⁵² M. T. Tran,⁴⁰ M. Tresch,⁴¹ A. Trisovic,³⁹ A. Tsaregorodtsev,⁶ P. Tsopelas,⁴² N. Tuning,^{42,39} A. Ukleja,²⁹ A. Ustyuzhanin,^{67,66} U. Uwer,¹² C. Vacca,^{16,39,j} V. Vagnoni,¹⁵ S. Valat,³⁹ G. Valenti,¹⁵ A. Vallier,⁷ R. Vazquez Gomez,¹⁹ P. Vazquez Regueiro,³⁸ C. Vázquez Sierra,³⁸ S. Vecchi,¹⁷ M. van Veghel,⁴² J. J. Velthuis,⁴⁷ M. Veltri,^{18,t} G. Veneziano,⁴⁰ M. Vesterinen,¹² B. Viaud,⁷ D. Vieira,² M. Vieites Diaz,³⁸ X. Vilasis-Cardona,^{37,e} V. Volkov,³³ A. Vollhardt,⁴¹ D. Voong,⁴⁷ A. Vorobyev,³¹ V. Vorobyev,³⁵ C. Voß,⁶⁵ J. A. de Vries,⁴² R. Waldi,⁶⁵ C. Wallace,⁴⁹ R. Wallace,¹³ J. Walsh,²⁴ J. Wang,⁶⁰ D. R. Ward,⁴⁸ N. K. Watson,⁴⁶ D. Websdale,⁵⁴ A. Weiden,⁴¹ M. Whitehead,³⁹ J. Wicht,⁴⁹ G. Wilkinson,^{56,39} M. Wilkinson,⁶⁰ M. Williams,³⁹ M. P. Williams,⁴⁶ M. Williams,⁵⁷ T. Williams,⁴⁶ F. F. Wilson,⁵⁰ J. Kimberley,⁵⁹ J. Wishahi,¹⁰ W. Wislicki,²⁹ M. Witek,²⁷ G. Wormser,⁷ S. A. Wotton,⁴⁸ K. Wraight,⁵² S. Wright,⁴⁸ K. Wyllie,³⁹ Y. Xie,⁶³ Z. Xu,⁴⁰ Z. Yang,³ H. Yin,⁶³ J. Yu,⁶³ X. Yuan,³⁵ O. Yushchenko,³⁶ M. Zangoli,¹⁵ M. Zavertyaev,^{11,u} L. Zhang,³ Y. Zhang,³ A. Zhelezov,¹² Y. Zheng,⁶² A. Zhokhov,³² L. Zhong,³ V. Zhukov,⁹ and S. Zucchelli¹⁵

(LHCb Collaboration)

¹Centro Brasileiro de Pesquisas Físicas (CBPF), Rio de Janeiro, Brazil

²Universidade Federal do Rio de Janeiro (UFRJ), Rio de Janeiro, Brazil

³Center for High Energy Physics, Tsinghua University, Beijing, China

⁴LAPP, Université Savoie Mont-Blanc, CNRS/IN2P3, Annecy-Le-Vieux, France

⁵Clermont Université, Université Blaise Pascal, CNRS/IN2P3, LPC, Clermont-Ferrand, France

⁶CPPM, Aix-Marseille Université, CNRS/IN2P3, Marseille, France

⁷LAL, Université Paris-Sud, CNRS/IN2P3, Orsay, France

⁸LPNHE, Université Pierre et Marie Curie, Université Paris Diderot, CNRS/IN2P3, Paris, France

⁹I. Physikalisches Institut, RWTH Aachen University, Aachen, Germany

¹⁰Fakultät Physik, Technische Universität Dortmund, Dortmund, Germany

¹¹Max-Planck-Institut für Kernphysik (MPIK), Heidelberg, Germany

¹²Physikalisches Institut, Ruprecht-Karls-Universität Heidelberg, Heidelberg, Germany

¹³School of Physics, University College Dublin, Dublin, Ireland

¹⁴Sezione INFN di Bari, Bari, Italy

¹⁵Sezione INFN di Bologna, Bologna, Italy

¹⁶Sezione INFN di Cagliari, Cagliari, Italy

¹⁷Sezione INFN di Ferrara, Ferrara, Italy

¹⁸Sezione INFN di Firenze, Firenze, Italy

¹⁹Laboratori Nazionali dell'INFN di Frascati, Frascati, Italy

²⁰Sezione INFN di Genova, Genova, Italy

²¹Sezione INFN di Milano Bicocca, Milano, Italy

²²Sezione INFN di Milano, Milano, Italy

²³Sezione INFN di Padova, Padova, Italy

²⁴Sezione INFN di Pisa, Pisa, Italy

²⁵Sezione INFN di Roma Tor Vergata, Roma, Italy

²⁶Sezione INFN di Roma La Sapienza, Roma, Italy

²⁷Henryk Niewodniczanski Institute of Nuclear Physics Polish Academy of Sciences, Kraków, Poland

²⁸AGH - University of Science and Technology, Faculty of Physics and Applied Computer Science, Kraków, Poland

²⁹National Center for Nuclear Research (NCBJ), Warsaw, Poland

³⁰Horia Hulubei National Institute of Physics and Nuclear Engineering, Bucharest-Magurele, Romania

³¹Petersburg Nuclear Physics Institute (PNPI), Gatchina, Russia

³²Institute of Theoretical and Experimental Physics (ITEP), Moscow, Russia

³³Institute of Nuclear Physics, Moscow State University (SINP MSU), Moscow, Russia

- ³⁴*Institute for Nuclear Research of the Russian Academy of Sciences (INR RAN), Moscow, Russia*
³⁵*Budker Institute of Nuclear Physics (SB RAS) and Novosibirsk State University, Novosibirsk, Russia*
³⁶*Institute for High Energy Physics (IHEP), Protvino, Russia*
³⁷*Universitat de Barcelona, Barcelona, Spain*
³⁸*Universidad de Santiago de Compostela, Santiago de Compostela, Spain*
³⁹*European Organization for Nuclear Research (CERN), Geneva, Switzerland*
⁴⁰*Ecole Polytechnique Fédérale de Lausanne (EPFL), Lausanne, Switzerland*
⁴¹*Physik-Institut, Universität Zürich, Zürich, Switzerland*
⁴²*Nikhef National Institute for Subatomic Physics, Amsterdam, The Netherlands*
⁴³*Nikhef National Institute for Subatomic Physics and VU University Amsterdam, Amsterdam, The Netherlands*
⁴⁴*NSC Kharkiv Institute of Physics and Technology (NSC KIPT), Kharkiv, Ukraine*
⁴⁵*Institute for Nuclear Research of the National Academy of Sciences (KINR), Kyiv, Ukraine*
⁴⁶*University of Birmingham, Birmingham, United Kingdom*
⁴⁷*H. H. Wills Physics Laboratory, University of Bristol, Bristol, United Kingdom*
⁴⁸*Cavendish Laboratory, University of Cambridge, Cambridge, United Kingdom*
⁴⁹*Department of Physics, University of Warwick, Coventry, United Kingdom*
⁵⁰*STFC Rutherford Appleton Laboratory, Didcot, United Kingdom*
⁵¹*School of Physics and Astronomy, University of Edinburgh, Edinburgh, United Kingdom*
⁵²*School of Physics and Astronomy, University of Glasgow, Glasgow, United Kingdom*
⁵³*Oliver Lodge Laboratory, University of Liverpool, Liverpool, United Kingdom*
⁵⁴*Imperial College London, London, United Kingdom*
⁵⁵*School of Physics and Astronomy, University of Manchester, Manchester, United Kingdom*
⁵⁶*Department of Physics, University of Oxford, Oxford, United Kingdom*
⁵⁷*Massachusetts Institute of Technology, Cambridge, Massachusetts, United States*
⁵⁸*University of Cincinnati, Cincinnati, Ohio, United States*
⁵⁹*University of Maryland, College Park, Maryland, United States*
⁶⁰*Syracuse University, Syracuse, New York, United States*
⁶¹*Pontifícia Universidade Católica do Rio de Janeiro (PUC-Rio), Rio de Janeiro, Brazil*
(associated with Universidade Federal do Rio de Janeiro (UFRJ), Rio de Janeiro, Brazil)
⁶²*University of Chinese Academy of Sciences, Beijing, China*
(associated with Center for High Energy Physics, Tsinghua University, Beijing, China)
⁶³*Institute of Particle Physics, Central China Normal University, Wuhan, Hubei, China*
(associated with Center for High Energy Physics, Tsinghua University, Beijing, China)
⁶⁴*Departamento de Física, Universidad Nacional de Colombia, Bogotá, Colombia*
(associated with LPNHE, Université Pierre et Marie Curie, Université Paris Diderot, CNRS/IN2P3, Paris, France)
⁶⁵*Institut für Physik, Universität Rostock, Rostock, Germany (associated with Physikalisches Institut, Ruprecht-Karls-Universität Heidelberg, Heidelberg, Germany)*
⁶⁶*National Research Centre Kurchatov Institute, Moscow, Russia*
(associated with Institute of Theoretical and Experimental Physics (ITEP), Moscow, Russia)
⁶⁷*Yandex School of Data Analysis, Moscow, Russia*
(associated with Institute of Theoretical and Experimental Physics (ITEP), Moscow, Russia)
⁶⁸*Instituto de Física Corpuscular (IFIC), Universitat de Valencia-CSIC, Valencia, Spain*
(associated with Universitat de Barcelona, Barcelona, Spain)
⁶⁹*Van Swinderen Institute, University of Groningen, Groningen, The Netherlands*
(associated with Nikhef National Institute for Subatomic Physics, Amsterdam, The Netherlands)

^aAlso at Università di Ferrara, Ferrara, Italy.

^bAlso at Università della Basilicata, Potenza, Italy.

^cAlso at Università di Milano Bicocca, Milano, Italy.

^dAlso at Università di Modena e Reggio Emilia, Modena, Italy.

^eAlso at LIFAELS, La Salle, Universitat Ramon Llull, Barcelona, Spain.

^fAlso at Università di Bologna, Bologna, Italy.

^gAlso at Università di Roma Tor Vergata, Roma, Italy.

^hAlso at Università di Genova, Genova, Italy.

ⁱAlso at Scuola Normale Superiore, Pisa, Italy.

^jAlso at Università di Cagliari, Cagliari, Italy.

^kAlso at Università di Padova, Padova, Italy.

^lAlso at Laboratoire Leprince-Ringuet, Palaiseau, France.

^mAlso at Universidade Federal do Triângulo Mineiro (UFTM), Uberaba-MG, Brazil.

ⁿAlso at AGH - University of Science and Technology, Faculty of Computer Science, Electronics and Telecommunications, Kraków, Poland.

^oAlso at Università degli Studi di Milano, Milano, Italy.

^pAlso at Hanoi University of Science, Hanoi, Viet Nam.

^qAlso at Università di Bari, Bari, Italy.

^rAlso at Università di Roma La Sapienza, Roma, Italy.

^sAlso at Università di Pisa, Pisa, Italy.

^tAlso at Università di Urbino, Urbino, Italy.

^uAlso at P. N. Lebedev Physical Institute, Russian Academy of Science (LPI RAS), Moscow, Russia.